OPEN ACCESS
JOURNAL OF ADVANCED DIELECTRICS
(2021) 2150031 (6 pages)

DOI: 10.1142/S2010135X21500314

Erbium upconversion luminescence from sol–gel derived multilayer porous inorganic perovskite film

M. V. Rudenko*, N. V. Gaponenko*,‖, E. B. Chubenko*, E. I. Lashkovskaya*, K. V. Shustsikava*, Yu. V. Radyush†, V. D. Zhivulko†, A. V. Mudryi†, M. Wang‡, E. V. Monaico§, M. V. Stepikhova¶ and A. N. Yablonskiy¶

*Belarusian State University of Informatics and Radioelectronics
P. Browki 6, 220013 Minsk, Belarus

†Scientific-Practical Materials Research Centre
of National Academy of Sciences of Belarus, 220072 Minsk, Belarus

‡Electronic Materials Research Laboratory (EMRL)
Key Laboratory of Education Ministry
International Center for Dielectric Research (ICDR)
Shaanxi Engineering Research Center of Advanced Energy Materials and Devices
School of Electronic and Information Engineering
Xi'an Jiaotong University, Xi'an, 710049, P. R. China

§National Center for Materials Study and Testing,
Technical University of Moldova
Stefan cel Mare Bd. 168, MD-2004, Chisinau, Republic of Moldova

¶Institute for Physics of Microstructures Russian Academy of Sciences
607680 Nizhny Novgorod, Russia

‖nik@nano.bsuir.edu.by

Received 15 October 2021; Revised 8 November 2021; Accepted 1 December 2021; Published 7 January 2022

Erbium-doped barium titanate ($BaTiO_3$:Er) xerogel film with a thickness of about 500 nm was formed on the porous strontium titanate ($SrTiO_3$) xerogel film on Si substrate after annealing at 800°C or 900°C. The elaborated structures show room temperature upconversion luminescence under 980 nm excitation with the photoluminescence (PL) bands at 523, 546, 658, 800 and 830 nm corresponding to $^2H_{11/2} \rightarrow {}^4I_{15/2}$, $^4S_{3/2} \rightarrow {}^4I_{15/2}$, $^4F_{9/2} \rightarrow {}^4I_{15/2}$ and $^4I_{9/2} \rightarrow {}^4I_{15/2}$ transitions of trivalent erbium. Raman and X-ray diffraction (XRD) analysis of $BaTiO_3$:Er\porous $SrTiO_3$\Si structure showed the presence of perovskite phases. Its excellent up-conversion optical performance will greatly broaden its applications in perovskite solar cells and high-end anti-counterfeiting technologies.

Keywords: Upconversion; barium titanate; erbium; sol–gel; porous films.

1. Introduction

Materials highly doped with trivalent erbium exhibit upconversion luminescence, in particular, conversion of infrared 980 nm and 1.54 μm radiation into visible. Erbium upconversion is the result of excited state absorption within any erbium ion or ion–ion interaction (energy transfer upconversion).[1] Efficiency of the upconversion depends on the host matrix, erbium concentration, method of synthesis, annealing conditions and other. Multilayer coatings with erbium upconversion are also very attractive for the development of solar cell technology, where thin films can be deposited on the backside of transparent solar cells to utilise sub-band gap photons.[2] In addition, in anti-counterfeiting technology, luminescent images can be obtained under infrared excitation as a multi-modal security mark.[3]

However, the mechanisms of enhancement for the conversion of infrared radiation into visible for erbium-doped coatings needs further development. Strong Stokes luminescence of erbium and other lanthanides was observed from xerogels embedded in mesoporous matrices like porous silicon[4,5] or porous anodic alumina[6,7] due to deep penetration of the sol through the porous layer and multiple scattering of exciting light. Nevertheless, application of meso- and macroporous silicon is limited to the silicon substrate, and on

‖Corresponding author.

the other hand, porous anodic alumina is transparent for the near-infrared radiation.[8] Recently, we reported that erbium upconversion was observed from erbium-doped $BaTiO_3$ ($BaTiO_3$:Er) sol–gel derived powder annealed at 1000°C with erbium concentration about 3 at.%.[9] In this work, we report on erbium upconversion from multilayer sol–gel derived spin coating comprising mesoporous $SrTiO_3$/$BaTiO_3$:Er structure annealed at 800°C and 900°C.

2. Experimental

Porous $SrTiO_3$ film was synthesized using water containing sol.[10] The sol was synthesized in the following way. First, titanium isopropoxide was dissolved in a mixture of ethylene glycol monomethyl ether and nitric acid to prevent gelation initiated by titanium isopropoxide. Then, strontium nitrate was dissolved in the distilled water, followed by the addition of ethylene glycol monomethyl ether. Finally, both solutions were mixed to obtain the sol. The sol was deposited by spinning at the rate of 2700 rpm for 30 s on monocrystalline silicon wafer. The samples were then dried at 200°C for 10 min and next film was identically deposited and dried. The deposition was repeated seven times in order to fabricate the film of an appropriate thickness. Final calcination was performed at 800°C for 40 min in air.

For the synthesis of barium titanate sol doped with erbium, titanium isopropoxide ($Ti(OC_3H_7)_4$), barium acetate ($Ba(CH_3COO)_2$), erbium acetate hydrate ($Er(CH_3COO)_3{\times}5.8\ H_2O$), acetylacetone ($CH_3COCH_2COCH_3$) and acetic acid ($CH_3COOH$) were used as starting components. The amounts of titanium isopropoxide and barium acetate were chosen so that the Ti/Ba ratio corresponded to the stoichiometric composition of the barium titanate in the films (i.e., Ti:Ba = 1:1). The mixture was stirred for 1 h with an electromechanical stirrer until all components were completely dissolved, resulting in a stable film-forming sol. $Er(CH_3COO)_3{\times}5.8\ H_2O$ was added to the $BaTiO_3$ sol to obtain 3 at.% of erbium in $BaTiO_3$ xerogel.[9]

Erbium-containing $BaTiO_3$ sol was deposited by spinning on previously deposited porous nanostructured strontium at 2000 rpm, then dried at 200°C for 10 min and annealed at 450°C for 30 min (heating rate of 10°C/min). Nine layers were prepared using this route. The samples were then heat treated at 800°C or 900°C with the heating rate of 8°C/min for 1 h. Additionally, erbium-doped $BaTiO_3$ coating was fabricated from the same sol under identical thermal processing on a series samples of mesoporous silicon 2–10 μm thick or polished monocrystalline silicon wafer.

The morphology of the experimental samples was examined with scanning electron microscope (SEM) S-4800 (Hitachi, Japan). XRD studies of the films were carried out with a DRON-3 diffractometer using monochromatic Cu Kα radiation with an exposition of about 2 s per 0.04° step at room temperature. Raman spectra were measured with 3D Scanning Laser Confocal Raman Microscope Confotec NR500 using 473 nm laser radiation for excitation. The measurements were performed at room temperature.

The focused 980 nm laser beam of a 200 mW diode module was used for the up-conversion photoluminescence (PL) measurements (excitation power density J ~ 10 W/cm^2). The resulting emission was focused on the entrance slit of a 0.6 m focal length monochromator equipped with 1200 gr/mm gratings, and the intensity was measured by Hamamatsu photomultiplier tube (R 9110) sensitive in the spectral region from 200 nm to 850 nm. The spectral resolution of the PL measurement system was ~ 0.6 nm. A lock-in-amplifier with mechanical chopping at a frequency of about 20 Hz was used for signal recovery.

3. Results and Discussion

Figure 1 shows the SEM images of the resulting $SrTiO_3$/Si structure. The SEM images of the 7-layer $SrTiO_3$ film with the estimated thickness of about 620 nm clearly reveal high porosity and highly developed surface.

As shown in Fig. 2, after a nine-fold deposition of the $BaTiO_3$:Er sol on the porous structure of strontium titanate and final heat treatment at 800°C a film of erbium-doped $BaTiO_3$ xerogel with a thickness of about 500 nm was generated on porous $SrTiO_3$. The total thickness of the xerogel structure is above one micron.

On the Raman spectra of the sample presented in Fig. 3, one can observe several bands corresponding to vibration modes of different materials [Table 1 (Refs. 11–16)].

Strong band located at 522 cm^{-1} belongs to single monocrystalline silicon substrate.[16] Crystalline silicon has symmetrical bonds with highly uniform angles and lengths. This results in only one first-order Raman active triply degenerate transverse optical phonon (TO) located at the Brillouin-zone centre. Double band at 948 and 988 cm^{-1} corresponds to second-order scattering from crystalline silicon (2TO).[16]

Two relatively sharp and strong bands with maxima located at 396 and 641 cm^{-1} can be attributed to TiO_2 with anatase crystalline structure[12] presumably from $SrTiO_3$ layer. They correspond to B_{1g} and E_g optically active TiO_2 vibration modes. The $A_{1g} + B_{1g}$ doublet usually observed on TiO_2 Raman shift spectra with maximum at 515 cm^{-1} also must be presented on the spectra, however it is hidden by intensive silicon (TO) vibration mode band.

Less intensive peaks located at 261, 281 and 729 cm^{-1} correspond to A(TO), E(TO+LO) and (E+A) (LO) vibration modes of crystalline $BaTiO_3$ phase with tetragonal crystal lattice structure. $BaTiO_3$ peak at 261 cm^{-1} also overlaps with $SrTiO_3$ (TO_3) O–Sr–O bridge bending vibration mode located at the same wavenumber.[10,12–14]

Figure 4 shows X-ray diffraction (XRD) spectrum of the obtained ($BaTiO_3$:Er)/$SrTiO_3$/Si structure. The diffraction line of 400 Si is clearly visible in the figure. The diffraction lines of perovskite are also indexed in the figure with the notation PS. The indices of the lines are given in cubic

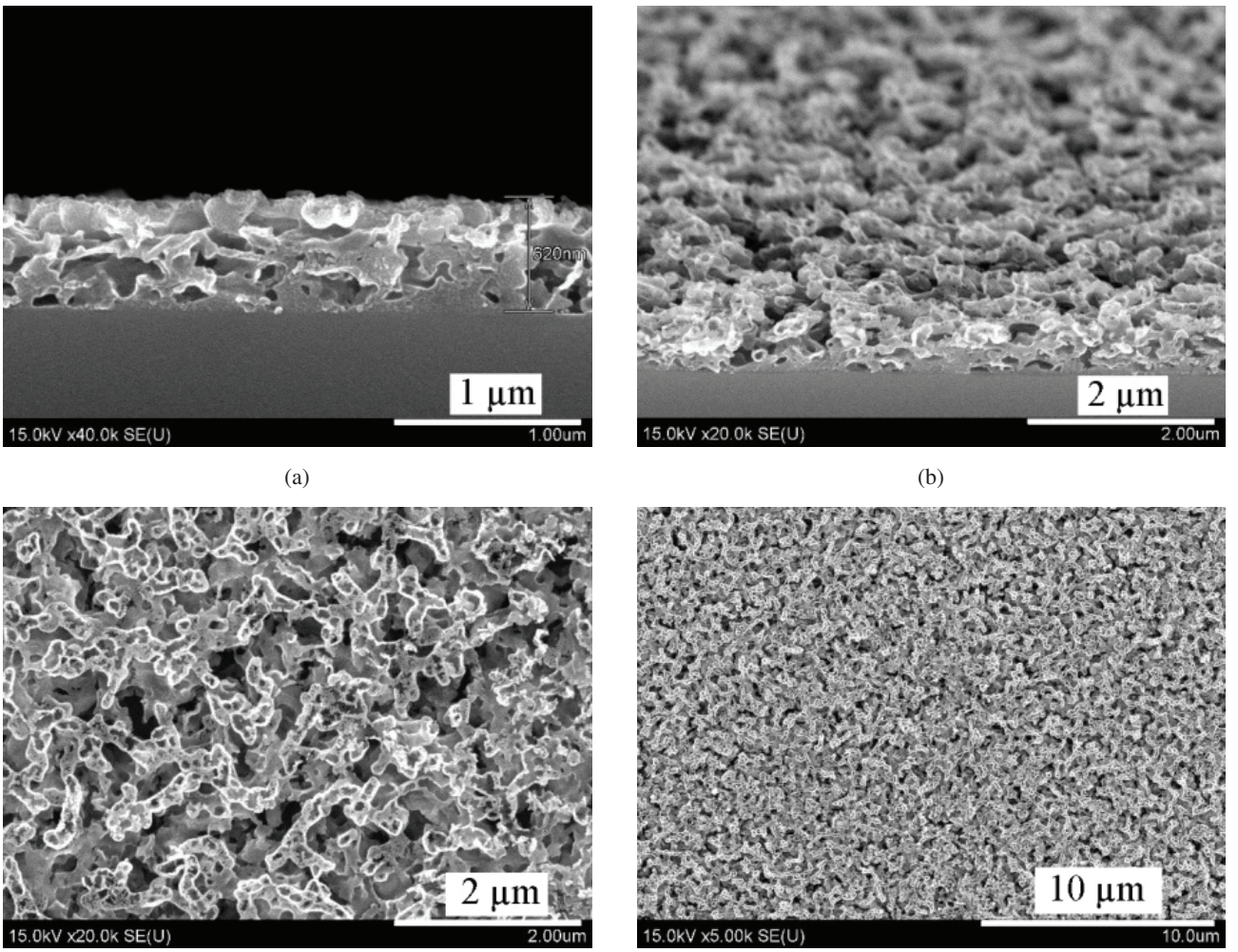

Fig. 1. SEM images of a porous nanostructured film formed on monocrystalline silicon containing seven layers of strontium titanate xerogel: (a) Cleaved edge. (b) Image taken at an angle of 70 to the sample surface. (c, d) Images of the surface at different magnifications.

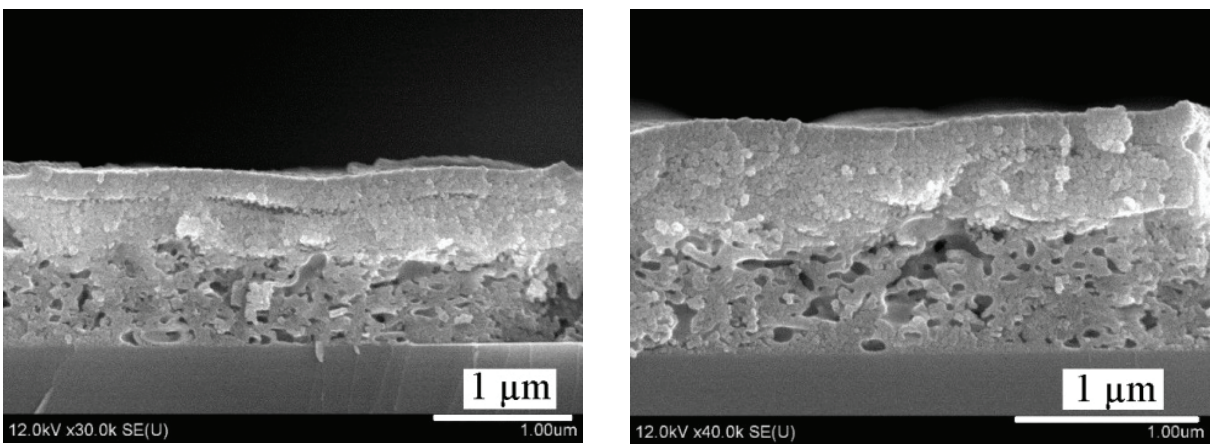

Fig. 2. SEM images of heterostructure ($BaTiO_3$:Er)/$SrTiO_3$/Si after annealing of each layer ($BaTiO_3$:Er) at 450°C and final annealing at 800°C.

Table 1. Position of Raman shift peaks of the porous xerogel film on silicon.

Peak position, cm^{-1}	Material	Mode	Reference
261	$BaTiO_3$	A (TO)	11
261	$SrTiO_3$	TO_3 (O–Sr–O bending)	12–14
281	$BaTiO_3$	E (TO+LO)	11
396	TiO_2 (anatase)	B_{1g}	15
522	Si	(TO)	16
641	TiO_2 (anatase)	E_g	15
729	$BaTiO_3$	E+A (LO)	11
948, 988	Si	(2TO) 2nd order	16

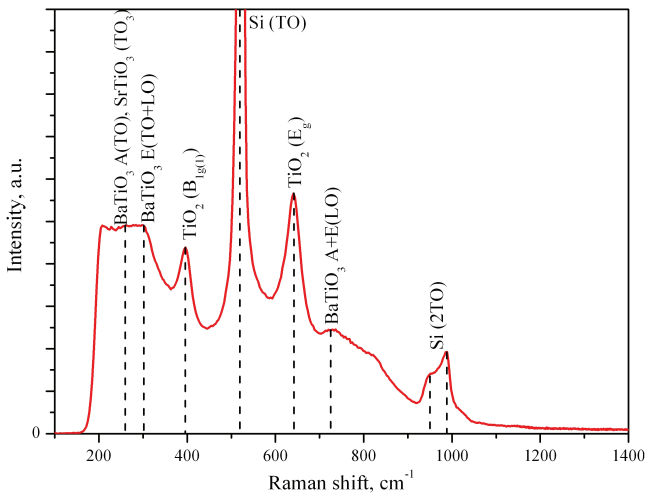

Fig. 3. Raman spectra of the porous xerogel film on silicon.

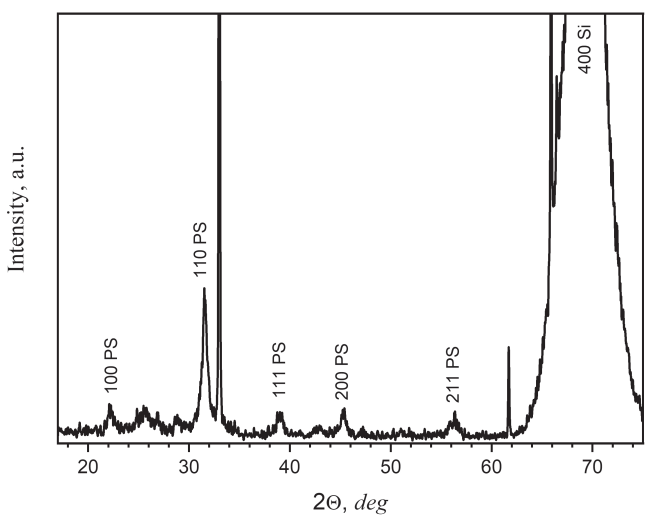

Fig. 4. XRD pattern in Cu Kα radiation of heterostructure ($BaTiO_3$:Er)/$SrTiO_3$/Si after annealing of each layer of $BaTiO_3$:Er at 450°C and final annealing at 800°C. The diffraction lines of perovskite are indexed with the notation PS.

approximation since the lines are blurred that makes it difficult to determine the crystal lattice structure more precisely. In addition, on the diffraction spectrum, there are rather narrow intensive lines at angles 32.96, 61.68, 65.87 and 66.44 whose origin has not been uniquely determined. These lines could be associated with erbium xerogel components.

Figure 5(a) shows the upconversion luminescence spectra from the heterostructure ($BaTiO_3$:Er)/$SrTiO_3$/Si. Figure 5(b) illustrates schematically energy level diagram of

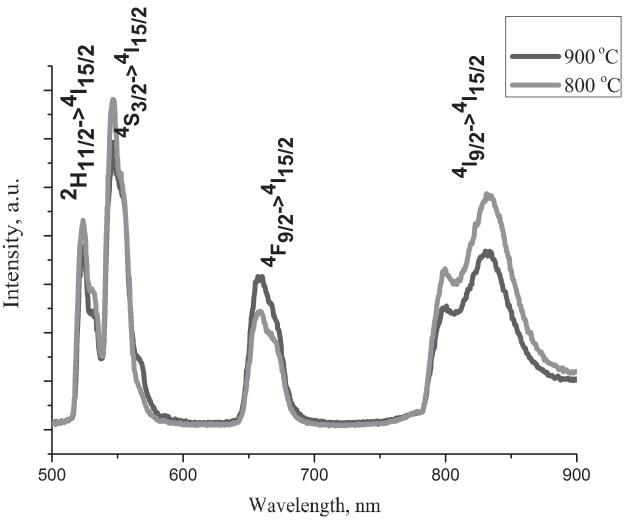

(a)

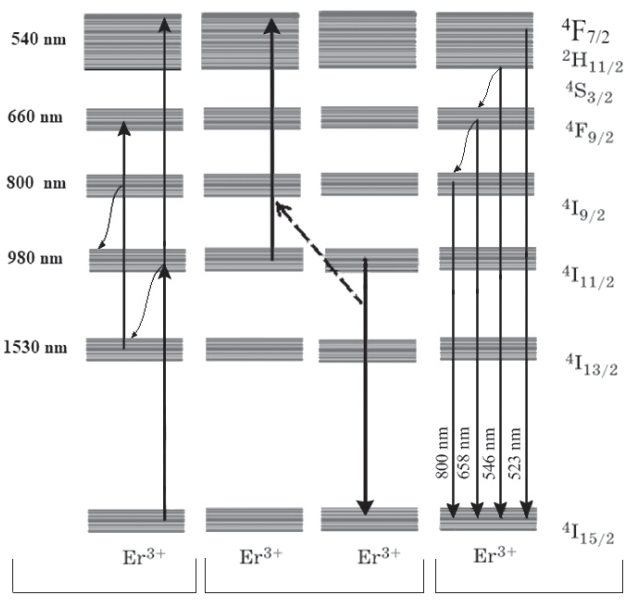

(b)

Fig. 5. (a) Upconversion luminescence spectra of ($BaTiO_3$:Er)/$SrTiO_3$/Si sample for the excitation wavelength 980 nm of a 200 mW diode module after annealing of each layer of $BaTiO_3$:Er at 450°C and final annealing at 800°C or 900°C. (b) Scheme of upconversion luminescence of Er^{3+} ions with separation the excited state absorption (left)), energy transfer upconversion between two neighboring ions (middle) and transitions from the excited states (right).

trivalent erbium with the Russell–Saunders notation of energy levels with sketch of their broadening due to Stark splitting in solids, possible excited state absorption within one erbium ion of energy quanta corresponding to the excitation wavelength 980 nm, the energy transfer (cooperative) upconversion between two neighboring erbium ions excited at $^4I_{11/2}$ level, and transitions (radiative and nonradiative) from the excited states of an erbium ion.[1,17–20] The spectra contain luminescence bands at 523, 546, 658, 800 and 830 nm due to $^2H_{11/2} \rightarrow {}^4I_{15/2}$, $^4S_{3/2} \rightarrow {}^4I_{15/2}$, $^4F_{9/2} \rightarrow {}^4I_{15/2}$ and $^4I_{9/2} \rightarrow {}^4I_{15/2}$ transitions of trivalent erbium. There is a slight splitting of the luminescence bands, which can be explained by the Stark effect. No erbium upconversion luminescence has been observed from the same multilayer $BaTiO_3$:Er xerogel film generated on mesoporous or monocrystalline silicon.

Two mechanisms may lead to population of the higher energy states levels with the excited photons corresponding to the wavelength 980 nm: excited states absorption and energy transfer (cooperative) upconversion. Excited state absorption may be the result of absorption the excited photons with one ion and transition of electrons from lower energy states to higher energy states: $^4I_{15/2} \rightarrow {}^4I_{11/2}$, $^4I_{11/2} \rightarrow {}^4F_{7/2}$, $^4I_{13/2} \rightarrow {}^4F_{9/2}$ (Fig. 5(b) left). The nonradiative transitions are shown in Fig. 5(b) with the wavy arrows. Energy transfer upconversion (Fig. 5(b) middle) is the case of ion–ion interaction of the excited neighboring erbium ions and observed for materials highly doped with erbium like $BaTiO_3$:Er xerogel described in this paper. Further work is needed to understand the predominant mechanism of erbium upconversion luminescence in the fabricated film structure ($BaTiO_3$:Er)/$SrTiO_3$/Si. We suppose that presence of porous strontium titanate layer coated with relatively dense erbium-doped barium titanate provides presence of erbium in meso- and macroporous volume of porous strontium titanate layer and in the intermediate between porous strontium titanate and more dense barium titanate layers. Thus, erbium containing inhomogeneous media comprising from the components with low and high refractive indices, in particular, air in the volume of the pores and islands of perovskites, is formed. The obtained inhomogeneous media with the size comparable to excitation wavelength 980 nm scatter the exciting light efficiently,[21] especially taking into account high value of the refractive index n of strontium titanate, $n \approx 2$ for the strontium titanate films depending on the fabrication technology and $n>2$ for the crystal (Refs. 22 and 23 and references therein). Enhanced scattering of exciting light leads to its effective absorption coefficient and absorption cross-section of erbium in porous perovskite media. To prove this, we can add, that no any upconversion luminescence is observed under the same experimental conditions from multilayer erbium-doped barium titanate xerogel films generated on monocrystalline silicon without porous strontium titanate layer. The lack of upconversion luminescence from mesoporous silicon could be understood assuming absence of erbium-doped inorganic perovskite phase within the porous silicon layer and fabrication of relatively thin $BaTiO_3$:Er xerogel film on its surface,[24] as well as considering possible change in the balance between the radiative and nonradiative recombination channels for erbium doped xerogel embedded in porous silicon or porous strontium titanate.

4. Conclusions

We described the sol–gel method of fabrication $BaTiO_3$:Er\porous $SrTiO_3$\Si multilayer film structures above one micron thick, which demonstrate room-temperature erbium upconversion luminescence at 523, 546, 658, 800 and 830 nm under the excitation wavelength 980 nm. XRD and Raman spectroscopy analyses confirm the formation of perovskite phases. Presence of porous layer ensures adhesion of thick luminescent film to the substrate. The technique does not require any organic template precursors in the sol for making the porous $SrTiO_3$ layer. This type of sol–gel derived structure could be generated on any substrate allowing heat treatment at 800°C, and raising of the annealing temperature to 900°C did not increase the obtained upconversion luminescence. The reason for the enhancement of the upconversion luminescence could be the multiple scattering of the excited light in the presense of porous strontium titanate layer. In what follows, additional enhancement of upconversion in the described erbium doped $BaTiO_3$/$SrTiO_3$ structure could be the result of its co-doping with the sensitizing Yb ions, that have an effective absorption cross-section. These film structures can be used as the convertors of infrared radiation into visible formed on the rear side of the solar cell or photodetector on silicon[2,20,25] and other semiconductors to utilize sub-bandgap photons and for the anti-counterfeiting technology[3] to get visible luminescent image under infrared excitation.

Acknowledgments

The authors would like to thank Prof. Alina Ponyavina from B. I. Stepanov Institute of Physics of National Academy of Sciences of Belarus for useful discussion. This research was funded by the grant T19-MLDG of State Committee on Science and Technology of the Republic of Belarus and grant 19.80013.50.07.03A/BL of the Republic of Moldova, grant X20P-388 of the Belarusian Republic Foundation for Fundamental Research and grant 20-52-00039 of the Russian Foundation for Basic Research.

References

[1]J. D. B. Bradley and M. Pollnau, Erbium-doped integrated waveguide amplifiers and lasers, *Laser Photon. Rev.* **5**, 368 (2011).
[2]A. Shalav, B. S. Richards and M. A. Green, Luminescent layers for enhanced silicon solar cell performance: Up-conversion, *Sol. Energy Mater. Sol. Cell.* **91**, 829 (2007).
[3]L. Liu, D. Yan, L. Xu, Z. Zhou, X. Sun, Y. Liu, X. Zong, E. Zhao, J. Ren, J. Zhang and H. Li, Intense and color-tunable upconversion through 980 and 1530 nm excitations, *J. Lumin.* **224**, 117306 (2020).

[4]A. M. Dorofeev, N. V. Gaponenko, V. P. Bondarenko, E. E. Bachilo, N. M. Kazuchits, A. A. Leshok, G. N. Troyanova, N. N. Vorozov, V. E. Borisenko, H. Gnaser, W. Bock, P. Becker and H. Oechsner, Erbium luminescence in porous silicon doped from spin-on films, *J. Appl. Phys.* **77**, 2679 (1995).

[5]W. Henley, Y. Koshka, J. Lagowski and J. Siejka, Infrared photoluminescence from Er doped porous Si, *J. Appl. Phys*. **87**, 7848 (2000).

[6]N. V. Gaponenko, I. S. Molchan, G. E. Thompson, P. Skeldon, A. Pakes, R. Kudrawiec, L. Bryja and J. Misiewicz, Photoluminescence of Eu-doped titania xerogel spin-on deposited on porous anodic alumina, *Sens. Actuators A* **99**, 71 (2002).

[7]N. V. Gaponenko, I. S. Molchan, O. V. Sergeev, G. E. Thompson, A. Pakes, P. Skeldon, R. Kudrawiec, L. Bryja, J. Misiewicz, J. C. Pivin, B. Hamilton and E. A. Stepanova, Enhancement of green terbium-related photoluminescence from highly doped microporous alumina xerogels in mesoporous anodic alumina, *J. Electrochem. Soc.* **149**, H49 (2002).

[8]N. V. Gaponenko, I. S. Molchan, S. V. Gaponenko, A. V. Mudryi, A. A. Lutich, J. Misiewicz and R. Kudrawiec, Luminescence of Eu^{3+} and Tb^{3+} ions in the structure microporous xerogel/mesoporous anodic aluminum oxide, *J. Appl. Spectroscopy* **70**, 59 (2003).

[9]N. V. Gaponenko, Yu. D. Karnilava, E. I. Lashkovskaya, V. D. Zhivulko, A. V. Mudryi, Yu. V. Radyush, B. A. Andreev, M. V. Stepikhova, A. N. Yablonskiy, S. A. Gusev, R. Subasri and D. S. Reddy, Radiative properties of up-conversion coatings formed on the basis of erbium-doped barium titanate xerogels, *Semiconductors* **55**, 965 (2021).

[10]M. Rudenko, N. Gaponenko, V. Litvinov, A. Ermachikhin, E. Chubenko, V. Borisenko, N. Mukhin, Y. Radyush, A. Tumarkin and A. Gagarin, Structural dependent Eu^{3+} luminescence, photoelectric and hysteresis effects in porous strontium titanate, *Materials* **13**, 5767 (2020).

[11]J. L. Parsons and L. Rimai, Raman spectrum of $BaTiO_3$, *Solid State Commun*. **5**, 423 (1967).

[12]M. L. Moreira, V. M. Longo, W. Avansi, Jr, M. M. Ferrer, J. Andrés, V. R. Mastelaro, J. A. Varela and É. Longo, Quantum mechanics insight into the microwave nucleation of $SrTiO_3$ nanospheres, *J. Phys. Chem.* **116**, 24792 (2012).

[13]Yu. I. Yuzyuk, Raman scattering spectra of ceramics, films, and superlattices of ferroelectric perovskites: A review, *Phys. Solid State*. **54**, 1026 (2012).

[14]L. F. da Silva, W. Avansi, Jr, J. Andres, C. Ribeiro, M. L. Moreira, E. Longo and V. R. Mastelaro, Long-range and short-range structures of cube-like shape $SrTiO_3$ powders: Microwave-assisted hydrothermal synthesis and photocatalytic activity, *Phys. Chem. Chem. Phys*. **15**, 12386 (2013).

[15]U. Balachandran and N. G. Eror, Raman spectra of titanium dioxide, *J. Solid State Chem*. **42**, 276 (1982).

[16]J. H. Parker, D. W. Feldman and M. Ashkin, Raman scattering by silicon and germanium, *Phys. Rev*. **155**, 712 (1967).

[17]A. Polman, Erbium implanted thin film photonic materials, *J. Appl. Phys.* **82**, 1 (1997).

[18]A. J. Kenyon, Recent developments in rare-earth doped materials for optoelectronics, *Prog. Quantum Electron.* **26**, 225 (2002).

[19]C. Lei, X.-H. Wei and F. Xu, Effect of Er substituting sites on upconversion luminescence of Er^{3+}-doped $BaTiO_3$ films, *Trans. Nonferrous Met. Soc. China* **22,** 1156 (2012).

[20]J. C. Goldschmidt and S. Fischer, Upconversion for photovoltaics – a review of materials, devices and concepts for performance enhancement, *Adv. Opt. Mater.* **3**, 510 (2015).

[21]C. F. Bohren and D. R. Huffman, *Absorption and Scattering of Light by Small Particles* (WILEY-VCH Verlag GmbH & Co. KGaA, 1998).

[22]A. I. Kulak, H. Sohrabi Anaraki, N. V. Gaponenko, L. S. Khoroshko, P. A. Kholov and T. F. Raichyonok, Optical characteristics of strontium titanate films formed by sol-gel method on quartz substrates, *J. Appl. Spectrosc.* **84**, 132 (2017).

[23]N. I. Stas'kov, A. B. Sotskii, L. I. Sotskaya, I. V. Ivashkevich, A. I. Kulak, N. V. Gaponenko, M. V. Rudenko and A. N. Petlitskii, Optical characteristics of strontium titanate films obtained by the sol–gel method, *Opt. Spectrosc*. **125**, 492 (2018).

[24]N. V. Gaponenko, Luminescence of lanthanides from xerogels embedded in mesoporous matrices, *Acta Phys. Pol.* **112**, 737 (2007).

[25]H. S. Anaraki, N. V. Gaponenko and V. A. Ivanov, Photocurrent in strontium titanate films on silicon substrates, *J. Appl. Spectrosc.* **82**, 857 (2015).